ISSN 2347-1921

Heat transfer of a nanofluid over a stretching sheet with velocity slip and temperature jump in porous medium in the presence of chemical reaction and radiation

Hunegnaw Dessie, D. Hymavathi, N.Kishan
Department of Mathematics, Osmania University Hyderabad 500007, T.S India.
hunegnawd@yahoo.com
Department of Mathematics, Mahatma Gandhi University, Nalgonda, T.S, India
Department of Mathematics, Osmania University, Hyderabad 500007, T.S, India.

ABSTRACT

In this study, heat transfer of a nanofluid over a stretching sheet with velocity slip and temperature jump in porous medium in the presence of chemical reaction and radiation is theoretically investigated. The governing partial differential equations with the corresponding boundary conditions are reduced to a set of ordinary differential equations via Lie group analysis. Numerical solutions of these equations are obtained by Runge-Kutta fourth order method along with shooting technique and the results obtained for different governing flow parameters are drawn graphically and their effects on velocity, temperature and concentration profiles are discussed. The reduced Nusselt number Nur and reduced Sherwood number Shr are presented in tabular form. It is noted that the reduced Nusselt number increases with the increase of Prandtl number but the reduced Sherwood number decreases. The effect of temperature jump parameter decreases the reduced Nusselt number and reduced Sherwood number.

Keywords: Porous medium; velocity slip; temperature jump; thermal radation; chemical reaction;shooting technique

Applied mathematics, Fluid dynamics.

0 MSC2010 No.: 34B15, 35 Q35, 76M20, 76R10, 76W05

Theoretical Approach method

Council for Innovative Research
Peer Review Research Publishing System
Journal: JOURNAL OF ADVANCES IN MATHEMATICS
Vol. 9, No. 6
www.cirjam.com , editorjam@gmail.com

ISSN 2347-1921

1. INTRODUCTION

The heat, mass, and momentum transfer in the laminar boundary layer flow over a stretching sheet are important from theoretical as well as practical point of view because of their wider applications to polymer technology and metallurgy. During many mechanical forming processes, such as extrusion, melt-spinning, cooling of a large metallic plate in a bath, manufacture of plastic and rubber sheets, glass blowing, continuous casting, and spinning of fibers, the extruded material issues through a die. The ambient fluid condition is stagnant but a flow is induced close to the material being extruded, due to the moving or stretching surface. In regions away from the slot, the flow may be considered to be of boundary layer type, although this is not true just near the slit. In all these cases, a study of the flow field and heat transfer can be of significant importance since the quality of the final product depends to a large extent on the skin friction coefficient and the surface heat transfer rate. First of all Sakiadis[1] investigated the boundary layer behavior on stretching surfaces and presented numerical solution for the sheet having constant speed. Extension to this problem where velocity is proportional to the distance from the slit was given by Crane [2]. Elsbashy et al. [3] considered flow and heat transfer in a porous medium over a stretching surface with internal heat generation and suction or injection. Mahapatra et al. [4] numerically investigated the MHD stagnation point flow and heat transfer over a stretching sheet. The unsteady mixed convection boundary layer flow in the region of stagnation-point on a vertical surface in a fluid-saturated medium is investigated by Nazar et al.[5]. Layek et al. [6] has reported heat and mass transfer boundary layer stagnation-point flow of an incompressible viscous fluid towards a heated porous stretching sheet embedded in a porous medium subject to suction/blowing with internal heat generation or absorption. Many authors discussed the boundary layer flows, stretching sheets and magnetic fields (Ishak et al. [7], Prasad et al.[8],Abe et al.[9],Prasad et al.[10]).

Nanofluids are the suspensions of nanometer-sized solid particles and fibers, which have been proposed as a route for surpassing the performance of heat transfer liquids currently available, such as water, oil and ethylene glycol mixture. Nanofluids have received the interest of many researchers recently because of their greatly enhanced thermal conductivity property. One can refer the works of Choi et al. [11a, 11b, 11c] regarding the thermal conductivity enhancement of the nanofluids available in the literature. Nowadays, the study of convective heat transfer in nanofluids has received much attention since cooling is one of the technical challenges faced by many industries including microelectronic, transportation, solid-state lighting and manufacturing and the idea of nanofluid has been proposed as a means of alleviating these challenges. Nield et al. [12] and Kuznetsov et al.[13] investigated the natural convective boundary layer flow of a nanofluid employing Buongiorno model. Malvandi [14] studied the unsteady flow of a nanofluid in the stagnation point region of a time dependent rotating sphere. Khan et al. [15] studied the boundary layer flow of a nanufluid past a stretching sheet with constant surface temperature using the model in which Brownian motion and thermophoresis effects were taken in to account. MHD boundary layer flow and heat transfer over a non-linearly permeable stretching/shrinking sheet in a nanofluid with suction effect, thermal radiation and chemical reaction is investigated by Hunegnaw et.al [16]. Hamad et al. [17] is investigated boundary layer stagnation-point flow towards a heated porous stretching sheet saturated with a nanofluid with heat absorption/generation and suction/blowing using Lie group analysis. Bachok et al. [18] analyzed three-dimensional stagnation-point flow and heat transfer in a nanofluid.

The thermal radiation effects become intensified at high absolute temperature levels due to basic difference between radiation and the convection and conduction energy-exchange mechanisms. In the context of space technology, some devices for space applications are designed to operate at high temperature levels in order to achieve high thermal efficiency. Hence, the effects of radiation are of vital importance when calculating thermal effects in the processes involving high temperatures. The radiation effects on MHD stagnation point flow of nanofluid over a stretching surface with convective boundary condition are studied by Akbar et al. [19]. Nadeem et al. [20] examined heat transfer analysis of water-based nanofluid over an exponentially stretching sheet. Makinde [21] reported the similarity solution for heat and mass transfer by MHD mixed convection stagnation point flow toward a vertical plate embedded in a highly porous medium with radiation and internal heat generation.

A few representative fields of interest, in which combined heat and mass transfer with chemical reaction effect plays an important role, are design of chemical processing equipment, formation and dispersion of fog, distribution of temperature and moisture over agricultural fields and groves of fruit trees, damage of crops due to freezing, food processing and cooling towers. For example, formation of smog is a first-order homogeneous chemical reaction. Chamkha [22] studied MHD flow over a uniformly stretched vertical permeable surface subject to a chemical reaction. Afify [23] analyzed the MHD free convective flow and mass transfer over a stretching sheet with a homogeneous chemical reaction of order n where n was taken to be 0, 1, 2, or 3. Kandasamy et al.[24] studied the effects of a chemical reaction on heat and mass transfer on a magnetohydrodynamic boundary layer flow over a wedge with ohmic heating and viscous dissipation in a porous medium. Patil et al.[25] considered the effects of chemical reaction on free convection flow of a polar fluid through a porous medium in the presence of internal heat generation.

In this paper the problem of heat transfer over a stretching sheet with velocity slip and temperature jump embedded in a nanofluid saturated porous medium in the presence of chemical reaction and radiation is considered. Lie's scaling` group transformations (also known as Lie group analysis or as symmetry analysis) can be used to obtain similarity transformations that can reduce a system of governing partial differential equations and associated boundary conditions to a system of ordinary differential equations. With this transformation, a third order and a second order ordinary

ISSN 2347-1921

differential equations corresponding to momentum, energy and concentration equations are derived. These equations are solved with the help of Runge Kutta fourth order along with shooting technique. The effects of different flow parameters on velocity, temperature and concentration profiles are investigated and analyzed with the help of graphical representation

2. FORMULATION OF THE PROBLEM

Consider the steady incompressible viscous fluid near a stagnation-point at a porous surface saturated by a nanofluid. Select a fluid stagnation point as the origin of the coordinate system, the $\bar{x}$-axis is the flat direction, that is, $\bar{y}$ =0. The flow region is confined to $\bar{y} > 0$. Along the $\bar{x}$-axis, there are two equal and opposite forces stretching flat so that the wall is stretched along the initial fixed direction. The stretching surface temperature and the nanoparticle fraction are deemed to have constant value T_w and C_w, respectively, while at a large value of $\bar{y}$, temperature and nanoparticale fraction have constant value T_∞ and C_∞ , respectively. The boundary layer equations governing the flow and temperature in presence of thermal radiation and chemical reaction are given as follows

$$\frac{\partial \bar{u}}{\partial \bar{x}} + \frac{\partial \bar{v}}{\partial \bar{y}} = 0 \tag{1}$$

$$\bar{u}\frac{\partial \bar{u}}{\partial \bar{x}} + \bar{v}\frac{\partial \bar{u}}{\partial \bar{y}} = \bar{U}(\bar{x})\frac{d\bar{U}}{d\bar{x}} + \nu\frac{\partial^2 \bar{u}}{\partial \bar{y}^2} + \frac{v}{k}(\bar{U}(\bar{x}) - \bar{u}) \tag{2}$$

$$\bar{u}\frac{\partial T}{\partial \bar{x}} + \bar{v}\frac{\partial T}{\partial \bar{y}} = \alpha\frac{\partial^2 T}{\partial \bar{y}^2} - \frac{1}{\rho c_p}\frac{\partial q_r}{\partial \bar{y}} + \tau\left\{D_B\frac{\partial T}{\partial \bar{y}}\frac{\partial C}{\partial \bar{y}} + \frac{D_T}{T_\infty}\left(\frac{\partial T}{\partial \bar{y}}\right)^2\right\} \tag{3}$$

$$\bar{u}\frac{\partial C}{\partial \bar{x}} + \bar{v}\frac{\partial C}{\partial \bar{y}} = D_B\frac{\partial^2 C}{\partial \bar{y}^2} + \frac{D_T}{T_\infty}\frac{\partial^2 T}{\partial \bar{y}^2} - k^*(C - C_\infty) \tag{4}$$

The slip boundary conditions for the physical problem under consideration are given by

$$\bar{u} = \bar{u}_w(\bar{x}) + \frac{2-\sigma_v}{\sigma_v}\lambda_0\left(\frac{\partial \bar{u}}{\partial \bar{y}}\right)_{\bar{y}=0} = b\bar{x} + \frac{2-\sigma_v}{\sigma_v}\lambda_0\left(\frac{\partial \bar{u}}{\partial \bar{y}}\right)_{\bar{y}=0}$$

$$\bar{v} = 0, T = T_w + \frac{2-\sigma_T}{\sigma_T}\left(\frac{2r}{r+1}\right)\frac{\lambda_0}{Pr}\frac{\partial T}{\partial \bar{y}}, C = C_w, \bar{y} = 0$$

$$\bar{u} \to \bar{U}(\bar{x}) = a\bar{x}, \quad T \to T_\infty, \quad C \to C_\infty \quad \text{as} \quad \bar{y} \to \infty \tag{5}$$

Where a and b are positive constants, σ_v is the tangential momentum accommodation coefficient, σ_T is the thermal accommodation coefficient, λ_0 is the molecular mean free path and r is the specific ratio. According to Rosseland's approximation [26], we can obtain $q_r = -\frac{4\sigma}{3k}\frac{\partial T^4}{\partial \bar{y}}$, where σ and k are Stefan-Boltzmann constant and absorption coefficient, respectively. We assume that the temperature variation T^4 may be expanded in a Taylor's series. Neglecting higher order terms and expanding T^4 about T_∞ ,we obtain, $T^4 \cong 4T_\infty{}^3\text{T-}3T_\infty{}^4$.

Now Eq. (3) can be written as

$$\bar{u}\frac{\partial T}{\partial \bar{x}} + \bar{v}\frac{\partial T}{\partial \bar{y}} = \alpha\frac{\partial^2 T}{\partial \bar{y}^2} + \tau\left\{D_B\frac{\partial T}{\partial \bar{y}}\frac{\partial C}{\partial \bar{y}} + \frac{D_T}{T_\infty}\left(\frac{\partial T}{\partial \bar{y}}\right)^2\right\} + \frac{16\sigma T_\infty{}^3}{3\rho c_p k}\frac{\partial^2 T}{\partial \bar{y}^2} \tag{6}$$

3. SIMILARITY TRANSFORMATIONS

The introduction of the following non-dimensional variables

$$x = \frac{\bar{x}}{\sqrt{v/b}}, = \frac{\bar{y}}{\sqrt{v/b}}, u = \frac{\bar{u}}{\sqrt{bv}}, v = \frac{\bar{v}}{\sqrt{bv}}, U = \frac{\bar{U}}{\sqrt{bv}} \tag{7}$$

Using Eq (7), Eqs (1)-(4) are transformed into the following no-dimensional variables equations

$$\frac{\partial u}{\partial x} + \frac{\partial v}{\partial y} = 0 \tag{8}$$

$$u\frac{\partial u}{\partial x} + v\frac{\partial u}{\partial y} = U\frac{dU}{dx} + \frac{\partial^2 u}{\partial y^2} + \frac{v}{kb}(U - u) \tag{9}$$

$$u\frac{\partial T}{\partial x}+v\frac{\partial T}{\partial y} \quad =\left(\frac{\alpha}{v}+\frac{16\sigma {T_\infty}^3}{3\rho v c_p k}\right)\frac{\partial^2 T}{\partial y^2}+.\frac{\tau}{v}\left[D_B\frac{\partial C}{\partial y}\frac{\partial T}{\partial y}+\frac{D_T}{T_\infty}\left(\frac{\partial T}{\partial y}\right)^2\right] \tag{10}$$

$$u\frac{\partial C}{\partial x}+v\frac{\partial C}{\partial y} \quad =\frac{D_B}{v}\frac{\partial^2 C}{\partial y^2}+\frac{D_T}{T_\infty v}\frac{\partial^2 T}{\partial y^2}-\frac{k^*}{b}(C-C_\infty) \tag{11}$$

We now introduce the following relations for u, v, θ and φ as follows

$$u=\frac{\partial \psi}{\partial y},\ \ v=-\frac{\partial \psi}{\partial x}\ \ ,\ \ \ \theta=\frac{T-T_\infty}{T_w-T_\infty}\ \text{and}\ \ \ \varphi=\frac{C-C_\infty}{C_w-C_\infty} \tag{12}$$

where ψ is the stream function

Then using equation (12), Equations. (9)- (11) can be written as

$$\frac{\partial \psi}{\partial y}\frac{\partial^2 \psi}{\partial x \partial y}-\frac{\partial \psi}{\partial x}\frac{\partial^2 \psi}{\partial y^2}=U\frac{dU}{dx}+\frac{\partial^3 \psi}{\partial y^3}+k_1\left(U-\frac{\partial \psi}{\partial y}\right) \tag{13}$$

$$\frac{\partial \psi}{\partial y}\frac{\partial \theta}{\partial x}-\frac{\partial \psi}{\partial x}\frac{\partial \theta}{\partial y}=\left(\frac{1}{Pr}+N\right)\frac{\partial^2 \theta}{\partial y^2}+Nb\frac{\partial \theta}{\partial y}\frac{\partial \varphi}{\partial y}+Nt\left(\frac{\partial \theta}{\partial y}\right)^2 \tag{14}$$

$$\left(\frac{\partial \psi}{\partial y}\frac{\partial \varphi}{\partial x}-\frac{\partial \psi}{\partial x}\frac{\partial \varphi}{\partial y}\right)=Le\frac{\partial^2 \varphi}{\partial y^2}+\frac{Nt}{Nb}\frac{\partial^2 \theta}{\partial y^2}-K\varphi \tag{15}$$

With boundary conditions

$$\frac{\partial \psi}{\partial y}=x+\frac{2-\sigma_v}{\sigma_v}\lambda_0\sqrt{\frac{b}{v}}\left(\frac{\partial^2 \psi}{\partial y^2}\right)_{y=0},\ \frac{\partial \psi}{\partial x}=0, \theta=1+\frac{2-\sigma_T}{\sigma_T}\left(\frac{2r}{r+1}\right)\sqrt{\frac{b}{v}}\frac{\lambda_0}{Pr}\frac{\partial \theta}{\partial y},\ \varphi=1,\ at\ \ y=0$$

$$\frac{\partial \psi}{\partial y}=\frac{a}{b}x, \qquad \theta\to 0, \quad \varphi\to 0 \qquad\qquad \text{as}\ y\to 0 \tag{16}$$

Scaling group transformation

A sophisticated and powerful method to obtain particular solutions to PDE is based on the study of their invariance with respect to one-parameter Lie group point transformations. The simplified form of the Lie-group transformation, namely the scaling group of transformations given by Hunegnaw et al. [27] is given by

$$\Gamma: \qquad x^*=xe^{\varepsilon\alpha_1}\ ,\quad y^*=ye^{\varepsilon\alpha_2}\ ,\quad \psi^*=\psi e^{\varepsilon\alpha_3}\ , U^*=Ue^{\varepsilon\alpha_4}$$
$$u^*=ue^{\varepsilon\alpha_5}, \qquad v^*=ve^{\varepsilon\alpha_6}\ , \qquad \theta^*=\theta e^{\varepsilon\alpha_7}\ \ \varphi^*=\varphi e^{\varepsilon\alpha_8} \tag{17}$$

Where α_1 , α_2 , α_3 , α_4, α_5 , α_6 and α_7 are transformation parameters.

Eq. (17) may be considered as a point-transformation which transforms coordinates $(x, y, \psi, u, v, \theta)$ to the coordinates $(x^*, y^*, \psi^*, u^*, v^*, \theta^*)$. Substituting equation (20) into (16)-(18), we obtain

$$e^{\varepsilon(\alpha_1+2\alpha_2-2\alpha_3)}\left(\frac{\partial \psi^*}{\partial y^*}\frac{\partial^2 \psi^*}{\partial x^*\partial y^*}-\frac{\partial \psi^*}{\partial x^*}\frac{\partial^2 \psi^*}{\partial {y^*}^2}\right)=e^{\varepsilon(\alpha_1-2\alpha_4)}U^*\frac{dU^*}{dx^*}+e^{\varepsilon(3\alpha_2-\alpha_3)}\frac{\partial^3 \psi^*}{\partial {y^*}^3}+$$
$$k_1\left(e^{\varepsilon(\alpha_1-\alpha_4)}\left(U^*-\frac{\partial \psi^*}{\partial y^*}\right)\right) \tag{18}$$

$$e^{\varepsilon(\alpha_1+\alpha_2-\alpha_3-\alpha_7)}\left(\frac{\partial \psi^*}{\partial y^*}\frac{\partial \theta^*}{\partial x^*}-\frac{\partial \psi^*}{\partial x^*}\frac{\partial \theta^*}{\partial y^*}\right)=\left(\frac{1}{Pr}+N\right)e^{\varepsilon(2\alpha_2-\alpha_7)}\frac{\partial^2 \theta^*}{\partial {y^*}^2}+$$
$$\mathrm{Nb}e^{\varepsilon(2\alpha_2-\alpha_7-\alpha_8)}\frac{\partial \theta^*}{\partial y^*}\frac{\partial \varphi^*}{\partial y^*} \tag{19}$$

$$e^{\varepsilon(\alpha_1+\alpha_2-\alpha_3-\alpha_8)}\left(\frac{\partial \psi^*}{\partial y^*}\frac{\partial \varphi^*}{\partial x^*}-\frac{\partial \psi^*}{\partial x^*}\frac{\partial \varphi^*}{\partial y^*}\right)=Lee^{\varepsilon(2\alpha_2-\alpha_8)}\frac{\partial^2 \varphi^*}{\partial {y^*}^2}-K\varphi^* e^{-\varepsilon\alpha_8}$$
$$+\frac{Nt}{Nb}e^{\varepsilon(2\alpha_2-\alpha_7)}\frac{\partial^2 \theta^*}{\partial {y^*}^2} \tag{20}$$

The boundary conditions are

$$\text{y= 0:}\ \ e^{\varepsilon(\alpha_2-\alpha_3)}\frac{\partial \psi^*}{\partial y^*}=x^*e^{-\varepsilon\alpha_1}+\frac{2-\sigma_v}{\sigma_v}\lambda_0\sqrt{\frac{b}{v}}e^{\varepsilon(2\alpha_2-\alpha_3)}\left(\frac{\partial^2 \psi^*}{\partial {y^*}^2}\right)_{y=0},\quad e^{\varepsilon(\alpha_1-\alpha_3)}\frac{\partial \psi^*}{\partial x^*}=0,$$

ISSN 2347-1921

$$\theta^* e^{-\varepsilon\alpha_7} = 1 + \frac{2-\sigma_T}{\sigma_T}\left(\frac{2r}{r+1}\right)\sqrt{\frac{b}{v}\frac{\lambda_0}{Pr}}\, e^{\varepsilon(\alpha_2-\alpha_7)}\frac{\partial\theta^*}{\partial y^*}, \qquad \varphi^* e^{-\varepsilon\alpha_8} = 1$$

$$y \to \infty:\ e^{\varepsilon(\alpha_2-\alpha_3)}\frac{\partial\psi^*}{\partial y^*} = \frac{a}{b}\, x^* e^{-\varepsilon\alpha_1}, \quad \theta^* e^{-\varepsilon\alpha_7} = 0, \quad \varphi^* e^{-\varepsilon\alpha_8} = 0 \qquad (21)$$

However, the system of Eqs. (18)- (20) together with boundary conditions of equation (21) remains invariant under the group of transformation Γ, if the following relations hold

$$\alpha_1 + 2\alpha_2 - 2\alpha_3 = \quad \alpha_1 - 2\alpha_4 = 3\alpha_2 - \alpha_3 = \alpha_1 - \alpha_4 = \alpha_2 - \alpha_3$$

$\alpha_1 + \alpha_2 - \alpha_3 - \alpha_7 = 2\alpha_2 - \alpha_7 = 2\alpha_2 - \alpha_7 - \alpha_8$

$\alpha_1 + \alpha_2 - \alpha_3 - \alpha_8 = 2\alpha_2 - \alpha_8 = -\alpha_8 = 2\alpha_2 - \alpha_7$

$$\alpha_2 - \alpha_3 = -\alpha_1 = 2\alpha_2 - \alpha_3\ ,\ \alpha_2 - \alpha_7 = -\alpha_7$$

This relation gives

$$\alpha_2 = 0,\ \alpha_3 = \alpha_1,\ \alpha_4 = \alpha_1,\ \alpha_5 = \alpha_1,\ \alpha_6 = 0,\ \alpha_7 = 0,\ \alpha_8 = 0$$

Thus the set reduces to a one parameter group of transformations:

$$x^* = xe^{\varepsilon\alpha_1}\ ,\quad y^* = y\ ,\qquad \psi^* = \psi e^{\varepsilon\alpha_1}\ , U^* = Ue^{\varepsilon\alpha_1}$$

$$u^* = ue^{\varepsilon\alpha_1},\qquad v^* = v\ ,\qquad \theta^* = \theta \quad \varphi^* = \varphi, \qquad (22)$$

Expanding by Taylor's method in powers of ε and keeping terms up to the order ε, we obtain

$$x^* - x = x\varepsilon\alpha_1,\quad y^* - y = 0,\ \psi^* - \psi = \psi\varepsilon\alpha_1, u^* - u = u\varepsilon\alpha_1,$$

$$U^* - U = U\varepsilon\alpha_1,\ \ v^* - v = 0, \theta^* - \theta = 0,\ \ \varphi^* - \varphi = 0$$

After differentials, we yield

$$\frac{dx}{\alpha_1 x} = \frac{dy}{0} = \frac{d\psi}{\psi\alpha_1} = \frac{d\theta}{0} = \frac{d\varphi}{0} \qquad (23)$$

Solving the above equation, we obtain

$$\eta = y,\qquad \psi = xf(\eta),\qquad \theta = \theta(\eta),\qquad \varphi = \varphi(\eta) \qquad (24)$$

Using these transformation equations (21) - (23) become

$$f''' + ff'' - f'^2 + \frac{a^2}{b^2} + k_1\left(\frac{a}{b} - f'\right) = 0 \qquad (25)$$

$$\left(\frac{1}{Pr} + N\right)\theta'' + f\theta' + Nb\theta'\varphi' + Nt\theta'^2 = 0 \qquad (26)$$

$$\varphi'' + Lef\varphi' + \frac{Nt}{Nb}\theta'' - K\varphi = 0 \qquad (27)$$

The corresponding boundary conditions become

$$f' = 1 + \gamma f''\ ,\ f = 0\ , \theta = 1 + \delta\theta'\ ,\ \varphi = 1 \quad \text{at} \quad \eta = 0$$
$$f' \to \frac{a}{b}\ ,\quad \theta \to 0,\quad \varphi \to 0 \qquad \text{at} \quad \eta \to \infty \qquad (28)$$

where prime denote the differentiation with respect to η. And $N = \frac{16\sigma {T_\infty}^3}{3\rho v c_p k}$ is thermal radiation pramter, $\gamma = \frac{2-\sigma_v}{\sigma_v}\lambda_0\sqrt{\frac{b}{v}}$ is the velocity slip parameter, $\delta = \frac{2-\sigma_T}{\sigma_T}\left(\frac{2r}{r+1}\right)\sqrt{\frac{b}{v}}\frac{\lambda_0}{Pr}$ is the jump temperature parameter,$k_1 = \frac{v}{bk}$ is the permeability parameter, $Pr = \frac{v}{\alpha}$ is the Prandtl number, $Le = \frac{v}{D_B}$ is Lewis number, $Nb = \frac{\tau D_B (C_w - C_\infty)}{v}$ is the Brownian motion parameter, $Nt = \frac{\tau D_T (T_w - T_\infty)}{v T_\infty}$ is the thermophoresis parameter, and $K = Le\frac{k^*}{b}$ is the chemical reaction parameter.

The quantities of practical interest, in this study, are the local Nusselt number Nu_x and the Sherwood number Sh_x which are defined as [15]

$$Nu_x = \frac{x q_w}{k(T_w - T_\infty)},\ Sh_x = \frac{x q_m}{D_B(C_w - C_\infty)},\ Re_x = \frac{x u_w(x)}{v}$$

The reduced Nusselt number Nur and the reduced Sherwood number Shr may be founded in terms of the dimensionless temperature at the sheet surface $\theta'(0)$ and the dimensionless concentration at the sheet surface $\varphi'(0)$,respectively.

$$Nur = {Re_x}^{-1/2} Nu_x = -\theta'(0) \qquad Shr = {Re_x}^{-1/2} Sh_x = -\varphi'(0)$$

Re_x is the local Reynolds number based on the stretching velocity $u_w(x)$, q_w is the surface(wall) heat flux, and q_m is the surface(wall) mass flux.

4. NUMERICAL METHOD FOR SOLUTION

The set of coupled non-linear ordinary differential equations (25) - (27) together with boundary conditions equation (28) are solved numerically by using Runge-Kutta fourth order technique along with shooting method. First of all, the higher order non-linear differential equations (25) - (27) are converted into simultaneous linear differential equation of first order and they are further transformed into initial value problem by applying the shooting technique. Now, defining new variables by the equations

$$f_1 = f,\ f_2 = f',\ f_3 = f'',\ f_4 = \theta,\ f_5 = \theta',\ f_6 = \varphi,\quad f_7 = \varphi' \tag{29}$$

The coupled higher order differential equations and the boundary conditions may be transformed to seven equivalent first order differential equations and boundary conditions, respectively, as given below

$$\left.\begin{aligned}
f_1' &= f_2 \\
f_2' &= f_3 \\
f_3' &= -f_1 f_3 + {f_2}^2 - \frac{a^2}{b^2} - k_1\left(\frac{a}{b} - f_2\right) \\
f_4' &= f_5 \\
f_5' &= \frac{\left(-\left(f_1 f_5 + Nb f_5 f_7 + Nt {f_5}^2\right)\right)}{\left(\frac{1}{Pr} + N\right)} \\
f_6' &= f_7 \\
f_7' &= -Le f_1 f_7 - \frac{Nt}{Nb}\left(\frac{\left(-\left(f_1 f_5 + Nb f_5 f_7 + Nt {f_5}^2\right)\right)}{\left(\frac{1}{Pr} + N\right)}\right) - K f_6
\end{aligned}\right\} \text{ System of equations.} \tag{30}$$

ISSN 2347-1921

The boundary conditions are

$$f_1(0) = 0, \quad f_2(0) = 1 + \gamma f_3(0), \quad f_4(0) = 1 + \delta f_5(0), \quad f_6(0) = 1$$
$$f_2(\infty) = \frac{a}{b}, \quad f_4(\infty) = 0, \quad f_6(\infty) = 0 \qquad (31)$$

Once the problem is reduced to initial value problem as the above, then it is solved by Runge-Kutta fourth order technique with systematic estimates of $f''(0)$, $\theta'(0)$ and $\varphi'(0)$ by the shooting technique. In this calculation the step size $\nabla\eta$=0.001 and six decimal accuracy as the criterion for convergence are used.

5. RESULTS AND DISCUSION

The computations have been carried out for the dimensionless velocity, temperature and concentration profiles for different flow parameters such as velocity ratio a/b, thermal radiation parameter$N$, the velocity slip parameter γ, the jump temperature parameter δ, the permeability parameter k_1, Prandtl number Pr, Lewis number Le, the Brownian motion parameter Nb, the thermophoresis parameter Nt and the chemical reaction parameter K. In order to verify the validity and accuracy of the present results, the values for the reduced Nusselt number Nur and the values of reduced Sherwood number Shr were compared with those reported by Zhegn et al. [27]. The comparison in the above cases is found to be in excellent agreement as shown in the Table 1. The values of reduced Nusselt number Nur and the values of reduced Sherwood number Shr for different values of flow parameters are tabulated in Table2. It is noted that from Table 2, both the values of the reduced Nusselt number Nur and reduced Sherwood number Shr decrease with increasing of the permeability parameter k_1, thermophoresis parameter Nt and the velocity slip parameter γ but both increase with increase of velocity ratio a/b. It is also pointed out from motion parameter Nb, chemical reaction K parameter and the temperature jump parameter δ. From the same table it can be observed that the increase of Prandtl number is to increase the value of the reduced Nusselt number, and is to decrease the reduced Sherwood number.

The dimensionless velocity, temperature and concentration profiles are shown graphically in figures 1-10 for different flow parameters. The influence of the Prandtl number Pr on the temperature profile is depicted in figure1. The increment of Prandtl number results in major effects on temperature field. The thermal boundary layer thickness reduces with Prandtl number and it happens due to decrease of thermal diffusivity for higher values of Pr. As a result , the temperature decreases with the increase of the Prandtl number as it is shown in the figure. Figure2 depicts the variation of concentration profiles for various Lewis numbers (Le). Lewis number defines the ratio of thermal diffusivity to mass diffusivity. It is used to characterize fluid flows where there is simultaneous heat and mass transfer by convection. From the figure, it is noted that the concentration decreases with an increase in Lewis number. The thermal radiation features in the energy conservation equation (26) are directly proportional to the conduction radiation parameter N. Thus; large value of N signifies a large radiation effect while N→0 corresponds to no radiation effect. The effect of conduction-radiation parameter (nonlinear Rosseland parameter,) on the dimensionless temperature profile in the boundary layer is shown in Figure 3a.Clearly as N is increased, thermal radiation contribution is raised and this is manifest with a considerable increase in temperature profile in the boundary layer. Therefore, for large values of N, thermal radiation is strong and this will correspond to maximum values of temperature and thicker thermal boundary layers. Evidently, the presence of strong thermal radiation flux is demonstrated to heat the thermal boundary layer markedly and is beneficial to materials processing systems where higher temperatures are often required to alter material characteristics.

ISSN 2347-1921

Table 1. Comparison of the results for the reduced Nusselt number $-\theta'(0)$ and reduced Sherwood number $-\varphi'(0)$ when Le=Pr=10 and $\gamma = \delta = N = \frac{a}{b} = k_1 = 0$

Nt	Nb	Nur	$Nur[28]$	Shr	$Shr[28]$
0.1	0.1	0.952432	0.95237	2.1294	2.12939
0.2	0.1	0.693173	0.69317	2.273956	2.27402
0.3	0.1	0.520085	0.52007	2.528542	2.52863
0.4	0.1	0.402584	0.40258	2.795041	2.79517
0.5	0.1	0.321059	0.32105	3.034980	3.03514
0.1	0.2	0.505579	0.50558	2.381840	2.38187
0.1	0.3	0.252298	0.25215	2.409994	2.41001
0.1	0.4	0.119406	0.11940	2.399624	2.39965
0.1	0.5	0.054253	0.05425	2.383547	2.38257

Table2. The values of reduced Nusselt number Nur and reduced Sherwood number Shr for different values Of the flow parameters

Pr	Le	N	K1	Nb	Nt	a/b	δ	γ	K	Nur	Shr
1	1	0.2	0.1	0.2	0.2	0.1	0.01	0.01	0.03	0.452933	0.364285
0.71	1	0.2	0.1	0.2	0.2	0.1	0.01	0.01	0.03	0.384911	0.413304
10	1	0.2	0.1	0.2	0.2	0.1	0.01	0.01	0.03	0.862102	0.053886
1	2	0.2	0.1	0.2	0.2	0.1	0.01	0.01	0.03	0.439966	0.726926
1	1	1	0.1	0.2	0.2	0.1	0.01	0.01	0.03	0.340302	0.445508
1	1	0.2	2	0.2	0.2	0.1	0.01	0.01	0.03	0.390175	0.319525
1	1	0.2	0.1	3	0.2	0.1	0.01	0.01	0.03	0.098811	0.620569
1	1	0.2	0.1	0.2	0.5	0.1	0.01	0.01	0.03	0.417266	0.052278
1	1	0.2	0.1	0.2	0.2	0.5	0.01	0.01	0.03	0.534374	0.461645
1	1	0.2	0.1	0.2	0.2	0.1	2	0.01	0.03	0.241534	0.481699
1	1	0.2	0.1	0.2	0.2	0.1	0.01	3	0.03	0.295452	0.283529
1	2	0.2	0.1	0.2	0.2	0.1	0.01	0.01	2	0.430609	1.509884

From figure 3b, it is observed that as N increases the nanoparticle volume fraction decreases away from the wall plate up to the crossing over point ($\eta \simeq 3.681$.) but after that it increases with increasing of N. Figure 4 displays the effects of permeability parameter k_1 on the velocity profile. It is observed from the figure that the velocity decreases with the increase of the permeability parameter. This is because the presence of the porous medium is to increase the resistance the fluid motion, which causes the fluid velocity to decrease. It is clear that values of Nb describe the strength of Brownian motion effects in figure 5a & 5b for temperature and nanoparticle volume fraction. The larger the values of Nb the greater will be the strength of Brownian motion effects. From figure5a it is observed that with an increase in Nb, the temperature profile and the thermal boundary thickness considerably increase. But the nanoparticle volume fraction profile significantly contracts as the Brownian motion parameter Nb increases as it is noticed from figure 5b. This is due to the fact that the increased Brownian motion of the nanoparticles serves to warm the boundary layer which leads to the effective movement of nanoparticles from the wall of the stretching sheet to the quiescent fluid and simultaneously intensifies particle deposition away from the fluid regime (onto the surface), thereby accounting for the reduced concentration magnitudes in

ISSN 2347-1921

figure 5b. Figures 6a & 6b show the effect of the thermophoresis parameter Nt on the temperature and nanoparticle volume fraction profiles.

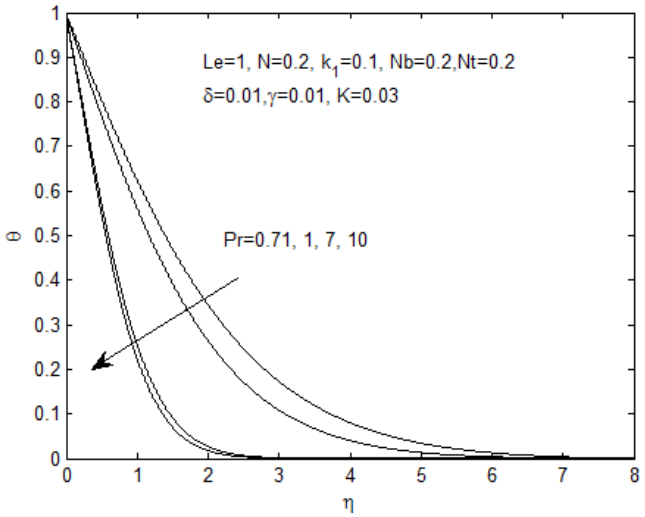

Figure 1. Temprature profiles for differet values of Prandtl number Pr

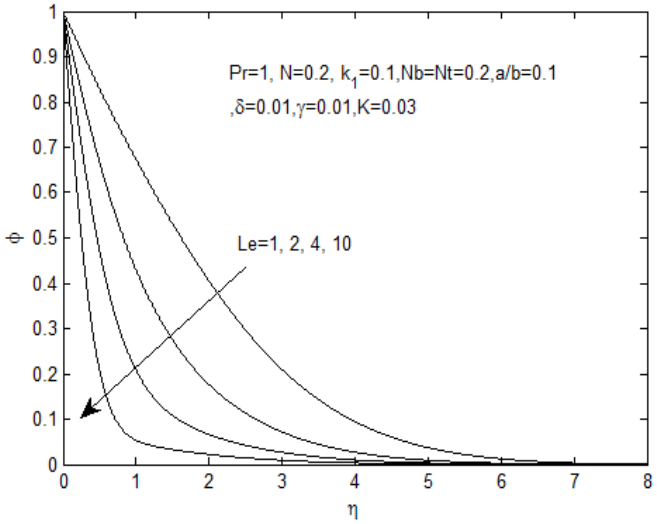

Figure2. Concentration profiles for different values of Lewis number Le

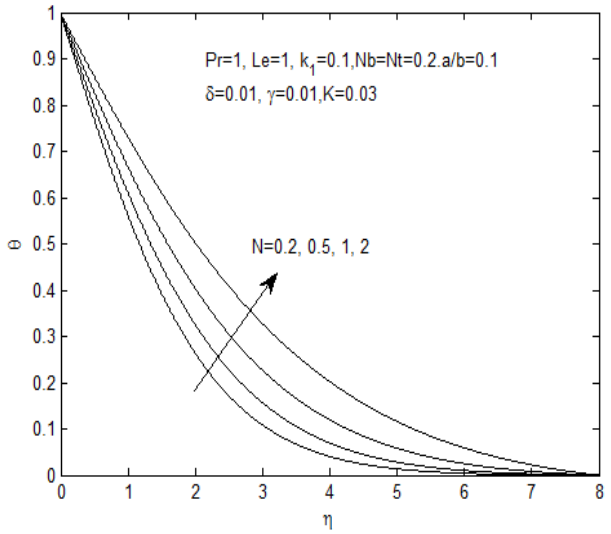

Figure 3a. Temprature profiles for different values of thermal radiation paramter N.

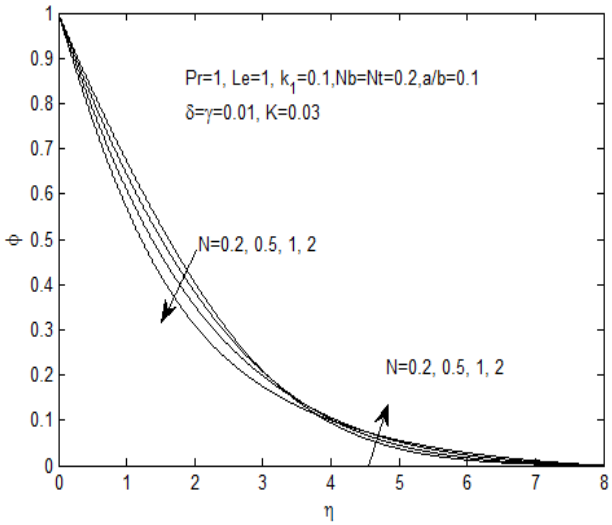

Figure 3b. Concentration profiles for different values of thermal radiation N

The thermophoretic force generated by the temperature gradient creates a fast flow away from the stretching surface. In this way more fluid is heated away from the surface, and consequently, as Nt increases, the temperature within the boundary layer increases. The fast flow from the stretching sheet carries with it nanoparticles leading to an increase in the nanoparticle volume fraction boundary layer thickness. Figure 7a shows that the boundary layer thickness decreases considerably as a/b increases. The increase in the value of a/b implies that free stream velocity increases in comparison to stretching velocity, which results in the increase in pressure and straining motion near stagnation point and hence thininig boundary layer takes place. The phenomenon of thinning boundary layer thus implies increased shear stress at the sheet. It is important to note for a/b =1, that there is no formation of boundary layer because the sheet velocity is equal to free stream velocity. It is seen from figures7b &7c that both the fluid temperature and concentration decrease due to increase of velocity ratio a/b. Effect of chemical reaction K on concentration profile is shown through figure.8.It is seen that the concentration of the fluid decreases with increase of chemical reaction parameter K.This is due the fact that the conversion of the species takes place as a result of chemical reaction and thereby reduces the concentration.

ISSN 2347-1921

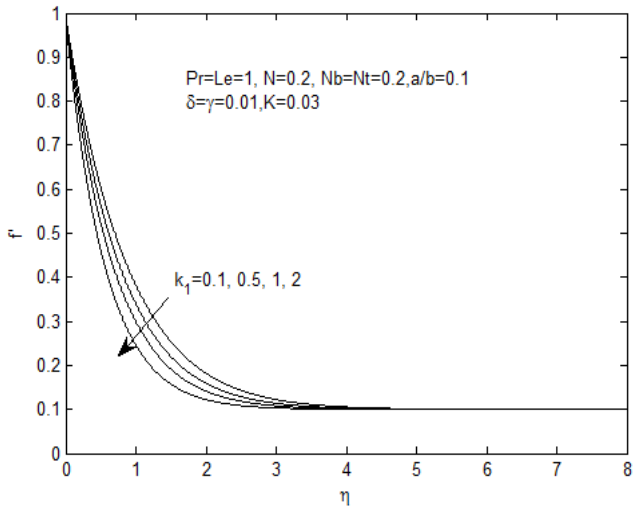

Figure4. Velocity profiles for different values of permeablity paramter k_1

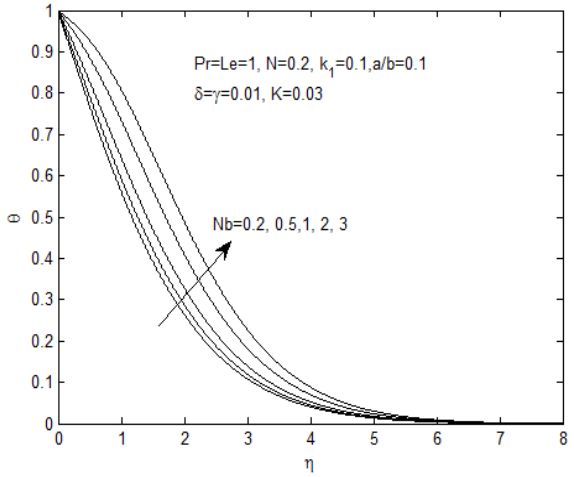

Figure 5a. Temprature profiles for different values of Brownian motion paramter Nb

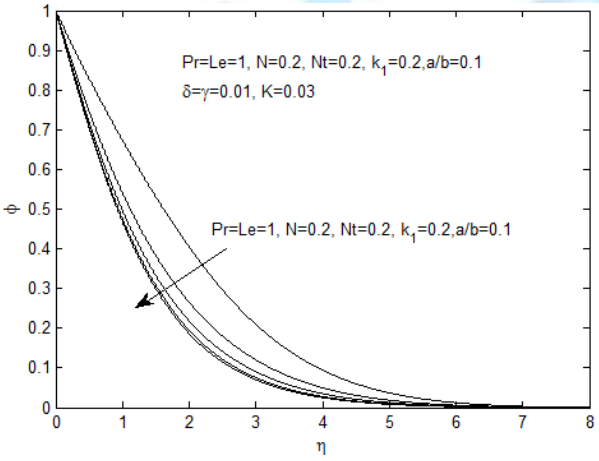

Figure5b. Concntration profiles for different values of Brownian motion paramter Nb.

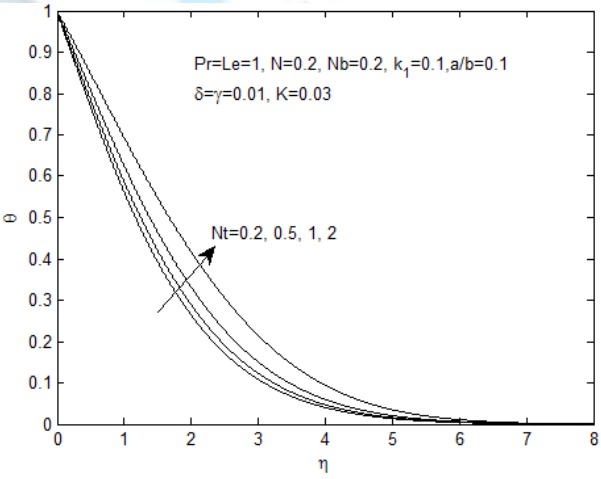

Figure 6a. Temprature profiles for diffenet values of thermopheresis paramter Nt

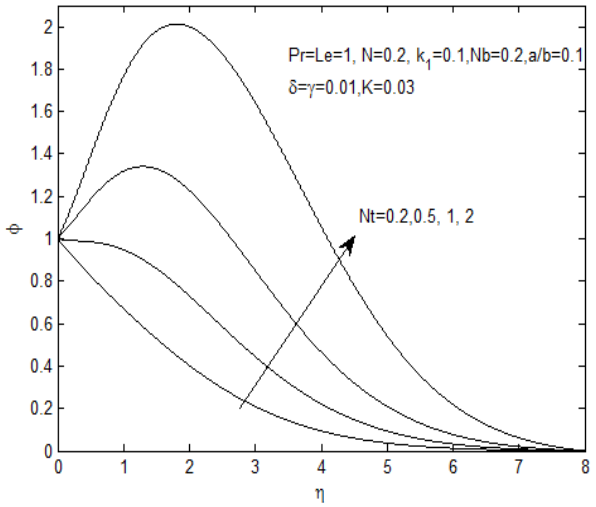

Figure6b. Concentration profiles for different values of thermopheresis paramter Nt

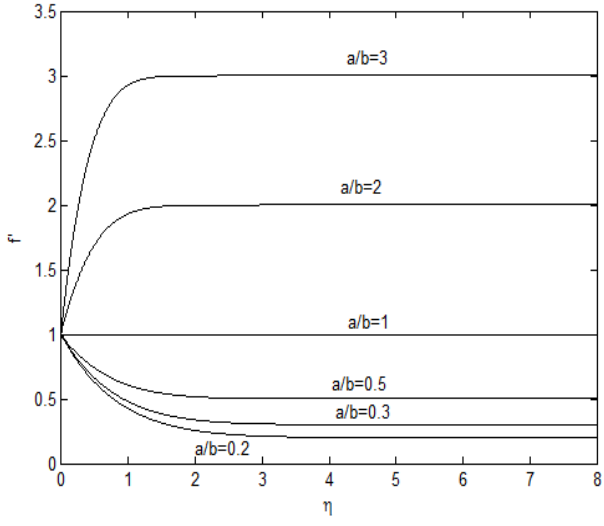

Figure 7a. velocity profiles for different values of velocity ratio a/b for Pr=1=Le,N=0.2, Nt=Nb=0.2,k_1=0.1,δ=γ=0.01 and K=0.03

The velocity profiles for a variation of velocity slip

parameter γ are shown in Figure9. It is noted from the figure that the increase of the velocity slip parameter is to decrease the velocity profiles. . Figures 10a & 10b show the variation of the temperature and concentration profiles for different values of temperature jump parameter δ. As seen in Figure 10a, the surface temperature and thickness of the

ISSN 2347-1921

thermal boundary layer decrease with the increase of temperature jump parameter δ. It is seen from figure 10b, the increase of temperature jump parameter is to decrease the concentration profiles.

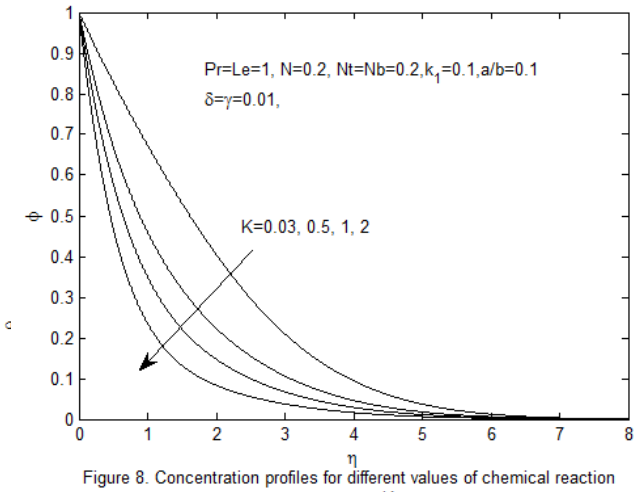

Figure 8. Concentration profiles for different values of chemical reaction paramter K

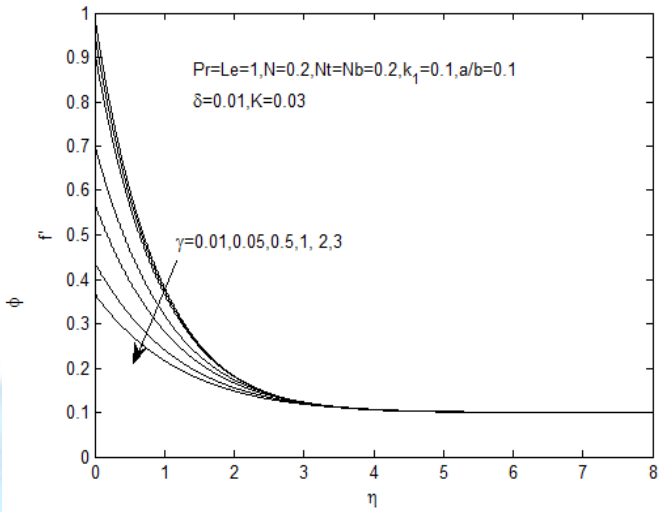

Figure9. velocity profiles for different values of velociy slip paramter γ

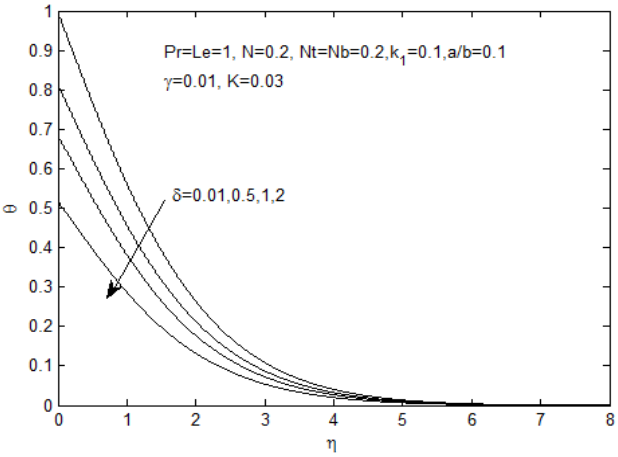

Figure10a. Temprature profiles for different values of temprature jump paramter δ

Figu

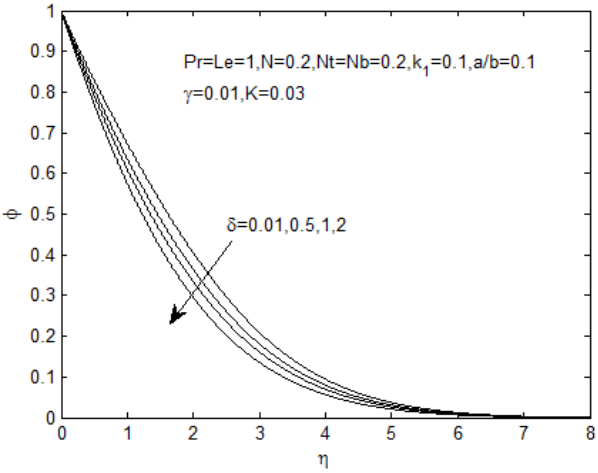

Figure10b. Concentration profiles for different values of temprature jump paramter δ

6. CONCLUSION

The present study gives the numerical solution for heat transfer over a stretching sheet with velocity slip and temperature jump embedded in a nanofluid saturated porous medium in the presence of chemical reaction and radiation. The model used for the nanofluid contains the effects of Brownian motion and thermophoresis efficient method of Lie group analysis is used to convert the partial differential equations in to non-linear ordinary differential equations. This procedure helps in removing the difficulties faced in solving the equations arising from the non-linear character of the partial differential equation. The resulting coupled non-linear ordinary differential equations are solved numerically using the Runge-Kutta fourth order along with shooting technique. The effects of governing flow parameters on the velocity, temperature and concentration fields are analyzed and discussed graphically. And the dependency of the reduced Nusselt number and Sherwood number on various flow parameters are illustrated in tabular form. Summary of the present work is listed as follows:

i. The temperature of the fluid increases and the concentration decreases with the increase of Brownian motion parameter ,

ii. An increase of the permeability parameter results in decreasing the velocity profiles.

iii. It is noted that the temperature profiles increase with the increase of the thermal radiation , whereas the concentration decrease up to crossing point and then increases

iv. An increasing of the chemical reaction parameter is to decrease the concentration profiles

v. The increase of temperature jump parameter causes to decrease temperature as well as the concentration profiles.

vi. The velocity profile decreases with the increase of velocity slip parameter.

REFRENCES

[1] Sakiadis, B.C. Boundary-layer behavior on continuous solid surfaces: I. Boundary-layer equations for two-dimensional and axisymmetric flow. AIChE Journal.7, 26–28(1961)

[2] Crane, L.J. Flow past a stretching plate, Journal of Applied Mathematics and Physics.21, 645–647(1970).

[3] Elbashbeshy, EMA, Basid MAA. Heat transfer in a porous medium over a stretching surface with internal heat generation and suction or injection. Appl Math Comput .158, 799–807(2004)

[4] Mahapatra T.R., A.S. Gupta, Magnetohydrodynamic stagnation-point flow towards a stretching sheet. Acta Mech. 152, 191–196(2001).

[5] Nazar R, Amin N, Filip D, Pop I, Unsteady boundary layer flow in the region of the stagnation-point on a stretching sheet. Int J Eng Sci. 42, 1241–1253(2004).

[6] Layek GC, Mukhopadhyay S, Samad SkA, Heat and mass transfer analysis for boundary layer stagnation-point flow towards a heated porous stretching sheet with heat absorption/generation and suction/blowing. Int Commun Heat Mass Transfer.34, 347–356(2007).

[7] Ishak A, Nazar R, Pop I, Magnaetohydrodynamic stagnation point flow towards a stretching vertical sheet. Magnaetohydrodynamic. 42, 17–30(2006).

[8] Prasad KV, Pal D, Umesh V, Rao NSP, The effect of variable viscosity on MHD viscoelastic fluid flow and heat transfer over a stretching sheet. Commun Nonlinear Sci Numer Simulat.15, 331–344(2010)

[9] Abel MS, Sanjayanand E, Nandeppanavar MM., Viscoelastic MHD flow and heat transfer over a stretching sheet with viscous and ohmic dissipations. Commun Nonlinear Sci Numer Simulat.13, 1808–1821(2008)

[10]. Prasad KV, Vajravelu K, Datti PS, The effects of variable fluid properties on the hydro-magnetic flow and heat transfer over a non-linearly stretching sheet. Int J Thermal Sci .49, 603–610(2010).

[11a] Choi S, Enhancing thermal conductivity of fluids with nanoparticle, Development and Applications of Non- Newtonian Flow. ASME FED- .231/MD. 66, 99-105(1995).

[11b] Choi S., Eastman, J.A.,, S.U.S.Li.S.Yu,W. and Thompson, L.J., Anomalously increased Effective thermal Conductivity of ethylene glycol-based nanofluids containing Copper Nanoparticles. Applied Physics Letters, 78(6), 718-720(2001)

[11c] Choi S., U.S., Zhang, Z.G., Yu, W.,Lockwoow, F.E., and Rule, E.A., Anomalous thermal Conductivities Enhancement on Nanotube Suspension. Applied Physics Letters.79, 2252-2254(2001)

[12]. Nield and A D.A, .V.Kuznetsov, The Cheng-Minkowyczproblem for natural convective boundary-layer flow in a porous medium saturated by a nanofluid. International Journal of Heat and Mass Transfer. 52(25-26), 5792–5795(2009)

[13] Kuznetsov A.V.and D.A.Nield, Natural convective boundary layer flow of a nanofluid past a vertical plate. Internation Journal of Thermal Sciences. 49(2), 243–247(2001).

[14] Malvandi A, The unsteady flow of a nanofluid in the stagnation point region of a time-dependent rotating sphere. THERMAL SCIENCE, 2013

[15] Khan WA, Pop I, Boundary layer flow of a nanofluid past a stretching sheet .Int J Heat Mass Transfer.53 , 2477-2483(2010).

[16] Hunegnaw D., Kishan N, MHD boundary layer flow and heat transfer over a non-linearly permeable

stretching/shrinking sheet in a nanofluid with suction effect, thermal radiation and chemical reaction.3, 1-9(2014).

[17] Hamad M.A.A, M.Ferdows, Similarity solution of the boundary layer stagnation-point flow towards a heated porous stretching sheet saturated with a nanofluid with heat absorption/generation and suction/blowing Commum Nonlinear Sci Numer Simulat .17,132-140(2012).

[18] Bachok N,A.Ishak,R.Nazar,I.Pop., Flow and heat transfer at a general three-dimensional stagnation-point flow in a nanofluid.Physica B .405,4914-4918(2010).

[19] Akbar N.S., S. Nadeem, R. Ul Haq, Z.H. Khan, Radiation effects on MHD stagnation point flow of nanofluid towards a stretching surface with convective boundary condition. Chin. J. Aeronaut. 26 (6), 1389–1397(2013).

[20]. Nadeem S., R. Ul Haq, Z.H. Khan, Heat transfer analysis of water-based nanofluid over an exponentially stretching sheet. Alexandria Eng. J. 53, 219–224(2014).

[21] Makinde O.D., Heat and mass transfer by MHD mixed convection stagnation point flow toward a vertical plate embedded in a highly porous medium with radiation and internal heat generation. Meccanica .47, 1173–1184(2012).

[22] Chamkha, A. J., MHD flow of a uniformly stretched vertical permeable surface in the presence of heat generation/absorption and a chemical reaction, International Communications in Heat and Mass Transfer. 30(3), 413–422(2003).

[23] Afify, A. A., MHD free convective flow and mass transfer over a stretching sheet with chemical reaction, Heat and Mass Transfer. 40(6), 495–500(2004).

[24] R. Kandasamy and P.G. Palanimani, Effects of chemical reactions, heat, and mass transfer on nonlinear magnetohydrodynamic boundary layer flow over a wedge with a porous medium in the presence of ohmic heating and viscous dissipation, J. Porous Media 10 (2007) 489–502

[25] Patil PM, Kulkarni PS, Effects of chemical reaction on free convective flow of a polar fluid through a porous medium in the presence of internal heat generation. Int J Thermal Sci (2008) .47:1043–1054

[26] Brewster MQ, Thermal radiative transfer properties. John Wiley and Sons, New York, 1992.

[27] Hunegnaw D., Kishan N., MHD effects on heat transfer over stretching sheet embedded in porous medium with variable viscosity, viscous dissipation and heat source/sink. Ain Shams Engineering Journal (2014), 5,967-977.

[28] Zheng L., Zhang C., Zhang X., Zhang J., Flow and radiation heat transfer of a nanofluid over a stretching sheet with velocity slip and temperature jump in porous medium.Journal of the Franklin Institute